JPP Journal of Pharmacy and Pharmacology

JPP 2007, 59: 241–250

Received January 26, 2006
Accepted May 22, 2006
DOI 10.1211/jpp.59.2.0010
ISSN 0022-3573

Characterization of the bulk properties of pharmaceutical solids using nonlinear optics – a review

Chris J. Lee, Clare J. Strachan, Peter J. Manson and Thomas Rades

Abstract

With the development of stable, compact and reliable pulsed laser sources the field of characterizing materials through their nonlinear optical response has bloomed. Second harmonic generation by non-centrosymmetric crystal structures has provided a new spectroscopic tool of potentially great utility in the pharmaceutical field. The nonlinear optical response of various materials provides a very sensitive technique for the characterization of pharmaceutically interesting bulk compounds and dispersions, and determining their concentrations. This work has potential application for in-line monitoring and quality control of pharmaceutical manufacturing. In this article we have presented an extensive review of the spectroscopic techniques that make use of the nonlinear optical response of solid media. Also, we have presented the results of our own work in this field.

Introduction

The physicochemical characterization of drugs (especially polymorphism and degree of crystallinity) is a necessary step in the development of medicines (Brittain 1995, 1999a). The use of combinatorial chemistry is likely to increase the number of drugs exhibiting polymorphism and the amorphous form, as drug molecules become larger (higher molecular weight) and contain more functional groups. Frequently these drugs will exhibit low dissolution controlled bioavailability (Biopharmaceutical Classification System (BCS) Class 2 (Amidon et al 1995; Center for Drug Evaluation and Research (CDER) 2000)). Different polymorphs of these drugs are likely to exhibit different absorption profiles and bioavailabilities (Haleblian 1975; Brittain 1999b; Bernstein 2002).

The dissolution rate of BCS Class 2 drugs may be improved by using an amorphous form (i.e. thermodynamically unstable form) of the active compound (Hancock & Zografi 1997) or a metastable crystalline form (Carstensen 1977). The stability of such forms is problematic and can result in the active compound crystallizing into the stable form upon processing and storage. On the other hand, stable polymorphs may also convert to unstable forms during processing. In addition, some solid state forms may be more easily processed than other forms (Haleblian & McCrone 1969; Haleblian 1975; Brittain 1999c). Thus, with therapeutic and formulation but also legal and commercial implications, it is crucial to be able to adequately identify and characterize drug polymorphism and crystallinity.

To be able to monitor and solve these problems throughout the drug discovery and production process, methods for the rapid, quantitative characterization of the solid state properties (crystallinity, polymorphism) in pure and mixed forms are desirable. Ideally several complimentary techniques should be used to provide a complete physicochemical picture of the compound. Previously, the primary investigative techniques have been X-ray diffraction (XRD) and thermal analysis (Brittain 1995). However, XRD is relatively insensitive to amorphous forms, while both XRD and thermal analysis are time consuming and not easily adaptable to in-line monitoring necessary for production processes. Various spectroscopic methods such as solid-state nuclear magnetic resonance (ss-NMR) and various vibrational spectroscopic techniques are becoming standard complementary methods (Tishmack et al 2003). ss-NMR, however, requires a very expensive apparatus, is difficult to adapt for in-line monitoring, and is quite slow. Vibrational spectroscopy on

Physics Department, University of Otago, P.O. Box 56, Dunedin, New Zealand

Chris J. Lee, Peter J. Manson

School of Pharmacy, University of Otago, P.O. Box 913, Dunedin, New Zealand

Clare J. Strachan, Thomas Rades

Division of Pharmaceutical Technology, University of Helsinki, Finland

Clare J. Strachan

Drug Discovery and Development Technology Centre, University of Helsinki, Finland

Clare J. Strachan

Correspondence: T. Rades, School of Pharmacy, University of Otago, P.O. Box 913, Dunedin, New Zealand. E-mail: thomas.rades@stonebow.otago.ac.nz

the other hand is rapid and relatively inexpensive (Colthup et al 1990; Kalinkova 1999; McCreery 2000).

Consequently, the development of novel optical spectroscopic techniques that allow rapid, qualitative and quantitative characterization of the solid state remains an area of active research in pharmaceutical and physical science disciplines. Spectroscopic methods that have been receiving particular attention for solid state analysis and their transitions include infrared, near infrared and Raman spectroscopy (Blanco et al 1998; Kalinkova 1999; Luner et al 2000; Aaltonen et al 2003; Strachan et al 2004a).

Recently, probing the optical nonlinear response of compounds to characterize various physicochemical properties has been the subject of increasing interest. The nonlinear optical properties of many materials depend not only on chemical structure but also on the symmetry class of the crystalline form of the compound. Even materials with similar chemical formulae that are in the same symmetry class may exhibit markedly different optical nonlinear responses. In addition the nonlinear optical response is sensitive to the particle size of the second harmonic active particles that make up the sample. Thus, as a spectroscopic analytical technique there is potential for an in-line monitoring tool that may provide a large data set that can be used rapidly to characterize a solid material. It is also possible, through surface symmetry breaking, to probe surface physicochemical properties. Processes such as adsorption and properties such as orientation of molecules at an interface all change the surface optical nonlinearity of materials that exhibit no bulk optical nonlinear response. As such the technique offers a potential tool in probing colloidal drug delivery systems as well.

The nonlinear optical response of most materials is very small and thus the field was only of cursory interest until the invention of the laser. The availability of high intensity radiation has renewed interest in nonlinear optics and it has been an area of active and fast paced scientific research ever since. Much of the work has and continues to be focused on device development (Tang & Cheng 1995; Akagawa et al 1997; Izumi et al 1998). These developments have led to many interesting spectroscopic devices in their own right (Baxter et al 1998; Miklos et al 2002). However, with the development of increasingly stable and compact laser sources it has become possible to focus on using the nonlinear optical properties as a probe. In this article results have been presented that show that the optical nonlinearity of bulk materials can be probed to provide information about relative concentration and phase composition.

Nonlinear optical spectroscopy can refer to any measurement that probes the optical nonlinearity of a sample. Such measurements encompass the intensity dependent refractive index, Raman scattering, Brillouin scattering or four wave mixing. The particular optical nonlinear responses we have focused on are the second-order optical nonlinearity which consists of sum and difference frequency generation (SFG and DFG) and the special case of SFG, second harmonic generation (SHG). In this paper we have introduced some of the theoretical concepts necessary to understand nonlinear optical interactions and have reviewed some recent experimental work on the characterization of bulk materials.

General nonlinear optical theory

Since nonlinear optics is a comparatively new topic in the pharmaceutical field, a short introduction to some of the concepts involved has been given. For more detailed information see Shen (1984) or Boyd (1992). An electromagnetic wave propagating through a medium induces a counteracting electric field (polarization wave) in the medium.

$$\tilde{P}(k,\omega) = \chi(k,\omega)\tilde{E}(k,\omega) \tag{1}$$

Where $\tilde{P}$ is the polarization, χ is the susceptibility of the medium, $\tilde{E}$ is the electric field of the electromagnetic wave while ω and k represent the frequency and wave vector of the electromagnetic wave, respectively. In this case the polarization refers not to the orientation of the field but the field induced by small displacements of charge within the medium. For most electric field intensities this response is linear, i.e. ω and k are the same for both the polarization and the electromagnetic waves. However, once the electromagnetic wave is sufficiently intense (10^6 Vm^{-1}) the response of the medium may no longer be linear. In this case the polarization wave will contain values of ω and k that are different from those of the electromagnetic wave and can generate new electromagnetic waves at these new frequencies and wave vectors. This is modelled by breaking the polarization up into separate parts (eqn 2).

$$\tilde{P}(k,\omega) = \tilde{P}^{(1)}(k,\omega) + \tilde{P}^{(2)}(k,\omega) + \tilde{P}^{(3)}(k,\omega) + \cdots \tag{2}$$

$$\tilde{P}^{(1)}(k,\omega) = \chi^{(1)}\tilde{E}(k,\omega) \tag{3}$$

$$\tilde{P}^{(2)}(k,\omega) = \chi^{(2)}(k = k_i + k_j, \omega = \omega_i + \omega_j)\ \tilde{E}(k_i,\omega_i) : \tilde{E}(k_j,\omega_j) \tag{4}$$

$$\tilde{P}^{(3)}(k,\omega) = \chi^{(3)}(k = k_i + k_j + k_l, \omega = \omega_i + \omega_j + \omega_l) : \tilde{E}(k_i,\omega_i)\ \tilde{E}(k_j,\omega_j)\tilde{E}(k_l,\omega_l) \tag{5}$$

Equations 3–5 represent the generating equations for increasing orders of optical activity. Equation 3 is the first (linear) term and corresponds directly to equation 1. Equation 4 is the second-order nonlinearity and it is generated by two electromagnetic waves whose frequencies and wave vectors sum to that of the original frequency and wave vector (this is necessary to conserve energy and momentum). Equation 5 shows the third-order nonlinearity and other orders can be added as required. The values of the nonlinear susceptibilities, $\chi^{(1)},\chi^{(2)},\chi^{(3)},\cdots$ are a summation of the optical nonlinearity of the constituent molecules. The summation process must take into account the orientation of the optical nonlinearity of

each molecule, thus the second-order optical nonlinearity of two molecules which are oriented 180° apart will cancel. It is this summation process that gives optical nonlinearity its dependence on both chemical formulation and physical structure.

The presence of electric field terms at frequencies and wave vectors different to the applied field indicate that the higher order polarization terms act as "sources" for new electromagnetic waves. Thus, the second-order electric field susceptibility, $\chi^{(2)}$, results in sum and difference frequency terms generated from two light fields. A special case of sum frequency generation (SFG) is second harmonic generation (SHG), where a single intense light field results in photons at twice the frequency of the illuminating light field. Since the susceptibility is a function of molecular structure and spatial organization, the response of the higher order polarization terms can be used as a probe to examine bulk, surface and molecular structure (Shen 1984; Janner 1998).

The polarization of the medium in response to the total applied electric field is a combination of the induced dipole moments of all the constituent atoms or molecules, and a full description of their behaviour depends on the quantum mechanical properties of the atomic or molecular system. However, much of the macroscopic, measurable behaviour can be obtained from a classical model with appropriate phenomenological additions. At the microscopic level, the response is usually expressed in terms of (hyper)polarizability tensors α, β... which relate the induced molecular dipole moment $\mu(t)$ to the electric field.

$$\mu(t) = \alpha : E(t) + \beta : E(t)E(t) + \gamma : E(t)E(t)E(t) + \cdots \tag{6}$$

Here α, β, ... are the molecular equivalent of the bulk susceptibilities described above.

The simplest, classical model of an atom consists of an electron cloud centered on a fixed positive nucleus, with the electron assumed to move in an anharmonic potential well. An externally applied electric field causes a small displacement of the electron cloud, producing on average a separation of the positive and negative charges in the atom and hence an electric dipole. The combination of all the microscopic electric dipoles produces the macroscopic polarization of the medium and hence electromagnetic radiation at new frequencies.

In this model (Shen 1984; Boyd 1992), the electron, with charge $-e$ and mass m, is treated as a classical particle displaced by a distance $x(t)$ from the fixed nucleus. The equation of motion for the electron is:

$$\frac{d^2x}{dt^2} + \gamma\frac{dx}{dt} + \omega_0^2 x + ax^{\eta} = -eE(t)/m. \tag{7}$$

The natural frequency w_0 of the harmonic motion is taken to be the frequency of the nearest absorption line of the molecule. The model also includes a damping force with coefficient γ which is related to the line width of the absorption feature. The force driving the oscillation is due to the applied electric field $E(t)$, assumed to be a number of monochromatic waves. The anharmonic term, ax^{η}, is included (Shen 1984; Boyd 1992) to represent the nonlinearity added to the basic harmonic oscillator model and for non-centrosymmetric materials $\eta = 2$. Without this term, the response of the oscillator is purely linear and no additional frequencies beyond those present in the incident field are generated.

Equation 7 cannot be solved directly, so a perturbative solution technique is used under the assumption that the anharmonic modification to the potential energy is small. The result is a dominant linear response with a series of corrective terms for each order of nonlinearity; the nonlinear terms show the presence of frequency mixing.

Although the classical anharmonic oscillator model predicts much of the form of the nonlinear optical response of an atom, it is a classical model and is expected to be incomplete. Perhaps the most obvious deficiency is that there is only a single resonance frequency, ω_0. The full quantum mechanical treatment overcomes these problems, and the interested reader may find a good example of such a treatment in Shen (1984).

The propagation of light in a nonlinear medium is also important when considering the interaction of light with the medium. Light propagation in a nonlinear medium is described by a wave equation in an insulator that includes the polarization as a source term and can be derived from Maxwell's equations. After making a number of assumptions about the illuminating pump and generated second harmonic light, the single partial differential equation of second-order derived from Maxwell's equations can be replaced by two first-order differential equations. These equations show that the build up of the second harmonic depends on the amplitude of the pump light and the decay of the pump light depends on the amplitude of both the second harmonic and the pump light. The efficiency of the power transfer between the pump and second harmonic is controlled by the wave vector mismatch between them, Δk:

$$\Delta k = k_{sh} - 2k_p \tag{8}$$

where subscript *sh* and *p* refer to the second harmonic and pump waves, respectively.

When $\Delta k \neq 0$ there is a characteristic length (called the coherence length) over which the second harmonic will build up. Decay will then occur over the following coherence length and the full cycle repeats every two coherence lengths, on average very little energy is transferred from the pump to the second harmonic. However, under some circumstances $\Delta k = 0$ (referred to as phase matching) can be achieved. In this case energy transfer between the fields is much more efficient. The wave vector mismatch is controlled by the wavelength dependent refractive index of the medium. Typically, the variation of refractive index with wavelength does not allow the phase mismatch to be zero when photon energy is conserved ($\omega_{sh} = 2\omega_p$). However, in an anisotropic material where k depends on the direction and polarization of the waves, phase matching can, in some cases, be achieved. In this case energy is efficiently transferred between waves over a characteristic distance determined by the material characteristics.

Spectroscopic applications of optical nonlinearity generally only allow the pump and second harmonic to interact over a distance that is short compared with that determined by the material characteristics, thus phase matching is not usually a consideration. However, phase matching can be significant in some forms of bulk spectroscopy where the aggregate distance over which the waves are allowed to mix can be quite long.

Optical nonlinearity in bulk turbid media

In much bulk nonlinear optical spectroscopy the sample is very disordered and strongly scattering. Thus, the description of propagation, energy transfer and phase matching must be approached statistically. This is well understood and we follow the approach of Sutherland (1996). The response of a single spherical particle, $I_{2\omega}$, goes as:

$$I_{2\omega} \propto d^2 L_c^2 \sin\frac{\pi r}{2L_c} \tag{9}$$

where $d = \frac{1}{2}\chi^{(2)}$, r is the particle radius and L_c is the coherence length. Application of equation 9 to a system of particles with an average size $\langle r \rangle$ depends on whether SHG can be a phase matched process within individual particles. In the case where SHG is phase matched, the response of the particles will be dominated by those particles with a favourable orientation to the laser beam. The coherence length becomes the average of:

$$L_c = \frac{\lambda_\omega}{4(n_{2\omega}^e - n_\omega^o)\sin\theta_{pm}(\theta - \theta_{pm})} \tag{10}$$

where λ_ω is the fundamental wavelength, θ is the laser angle of incidence relative to the optical axis of the particle* and n^o and n^e are the refractive indices experienced by orthogonally polarized beams of light while θ_{pm} corresponds to the phase matching angle. Provided that $\langle r \rangle \gg \Lambda_{pm}/\sin\theta_{pm}$ the second harmonic response goes as:

$$I_{2\omega} \propto d_{eff}^2 L \Lambda_{pm} \tag{11}$$

where $L\Lambda_{pm}$ is the effective bulk sample length over which efficient SHG can occur and d_{eff} is the combination of d tensor elements in the phase-matching direction. In a non-scattering medium $L\Lambda_{pm}$ would be given by the interaction length discussed earlier, and if the system was immersed in an index matching fluid replacing $L\Lambda_{pm}$ with the interaction length would be a valid approximation. When $\langle r \rangle \leq \Lambda_{pm}/\sin\theta_{pm}$, each particle emits some fraction of second harmonic, which is partially correlated with that emitted by the others. The nonlinear polarization can then be treated like a one dimensional random walk. The result is simply proportional to the size of particles:

$$I_{2\omega} \propto d_{eff}^2 \frac{L}{\langle L_c \rangle}\frac{\langle r \rangle}{\langle L_c \rangle} \tag{12}$$

where L is the path length of the sample. If the particles cannot be phase-matched and are much larger than the coherence length, then the response of each particle has no phase coherence with any other. In this case simply sum the intensities by multiplying the single particle response (eqn 9) by the number of particles. Since the orientation of the particles is random d must be averaged as well. The resulting response is:

$$I_{2\omega} \propto \langle d^2 \rangle L \langle L_c \rangle \frac{\langle L_c \rangle}{\langle r \rangle} \tag{13}$$

where $\langle L_c \rangle$ is the average coherence length given by the material characteristics of the particles. For the case of $\langle r \rangle \leq \langle L_c \rangle$ the same argument as used for equation 12 can be applied but with d_{eff}^2 replaced with $\langle d^2 \rangle$.

$$I_{2\omega} \propto \langle d^2 \rangle \frac{L}{\langle L_c \rangle}\frac{\langle r \rangle}{\langle L_c \rangle} \tag{14}$$

thus the response of a system of powdered substances theoretically will have particle size dependence similar to that shown in Figure 1. In reality the response is smooth due to the non-zero size distribution of particles.

The results presented in equations 11–14 have three common assumptions. These assumptions are that the particles are all of a single species and polymorph, that the gaps between particles are much smaller than $\langle L_c \rangle$ and that the particles are all immersed in an index matching fluid. In the next section we have presented experimental results showing some of the applications of nonlinear optical spectroscopy to characterization of bulk turbid media.

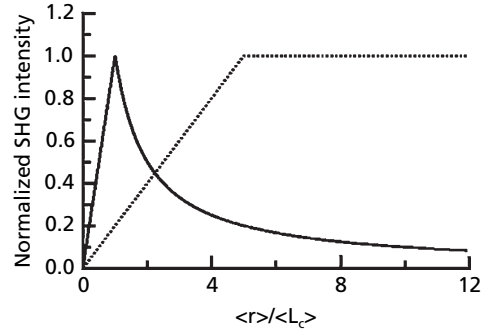

Figure 1 Theoretical response of phase-matched (dashed line) and non-phase-matched (solid line) particles as a function of size. In a real experiment these are smooth curves because one has a distribution of particles sizes in each sample and the phase-matched curve will be much higher on the abscissa than the non-phase-matched curve.

*The optical axis of a material is defined by the direction for which the refractive index is independent of the polarization of the electrical field of the light wave.

Second harmonic generation in bulk

Non-pharmaceutical materials

SHG was initially used to characterize non-pharmaceutical materials; however, such research illustrates potential applications in the pharmaceutical setting, and is thus worthy of review in this context. LeCaptain & Burglund (1999) used SHG to monitor the phase and growth of a non centrosymmetric crystalline material. They observed spontaneous nucleation, the induction time (the time taken for the first crystals to form) and the dynamical behaviour of crystallization of a supersaturated dihydrogen phosphate solution. Similar but more qualitative studies were performed on β-lactose and lysine m-HCl (LeCaptain & Burglund 1999).

Phase changes in bulk media have been observed using SHG as a probe. Henson et al (1999) observed the β–δ phase transition of HMX (octahydro-1,3,5,7-tetranitro-1,3,5,7-tetraocine) which is an explosive. The β form of HMX is stable but the material rapidly decomposes on transition to the δ phase. Heating β-HMX induces a phase change to the δ form which then rapidly decomposes, producing the explosive reaction associated with it. By carefully heating the sample with a CO_2 laser and irradiating the sample with a pulsed Nd:YAG laser the authors were able to observe the rapid β–δ phase transition by monitoring the intensity of the light scattered from the sample at the second harmonic of the Nd:YAG wavelength. Such phase transitions are thought to occur in other explosives and this has since been observed using nonlinear optical techniques (Son et al 1999).

Critical exponents associated with phase transitions can be measured using SHG. Fokin et al (2004) measured the phase and switching characteristics of liquid crystals by monitoring the intensity of SHG signal transmitted by the liquid crystal cell. By changing the cell voltage and/or temperature a liquid crystal phase transition could be induced and the dynamics of the transition monitored. These measurements were sufficient to determine the critical exponents associated with the phase transition and in addition were able to determine that the phase transition dynamics were not uniform throughout the cell.

In our group, we have focused on using bulk SHG in powders to determine the relative concentration of binary solid-state mixtures. The speed of an SHG measurement makes it a promising candidate for in-line monitoring during drug production and these initial experiments were designed to test the feasibility of SHG spectroscopy for such a purpose.

Initial work was limited to quartz and glass since it is known that quartz has an optical nonlinearity, while glass by virtue of its amorphous state has no second-order nonlinear response. Quartz and glass are both primarily composed of silicon dioxide, SiO_2. Quartz has very few impurities and the samples employed were crystallized in the trigonal form, belonging to space group, $P3_12_1$. Unlike quartz, glass has various metal impurities that fluoresce, complicating SHG detection. Pyrex was the preferred choice of glass because it contains approximately 4% boron, and a small amount of fluorescing components such as sodium, while ordinary window glass contains more sodium and also calcium (Sullivan & Taylor 1919).

The intensity of scattered second harmonic light across the spectral range of 392 to 692 nm was recorded for both quartz and Pyrex samples (see Figure 2). The response of quartz was limited to exactly the expected SHG signal (532 nm) within the limits of the spectrometer. Pyrex showed no dominant spectral peaks but emitted a small amount of radiation over the entire measurement range. The response from Pyrex decayed with time, suggesting that Pyrex exhibited some two-photon fluorescence, which was probably due to sodium and could be avoided by delaying measurement for approximately 30 s (Strachan 2005).

The size dependence of the SHG signal from quartz and Pyrex was tested over the size ranges of approximately 45–250 μm (see Figure 3). SHG measurements of quartz samples could not detect any particle size dependence over the range investigated, probably because the particle size range of quartz was sufficiently large ($>> L_c$). The insensitivity of the measurement to size dependence is an advantage for quantitative analysis of pharmaceutical polymorphism or crystallinity.

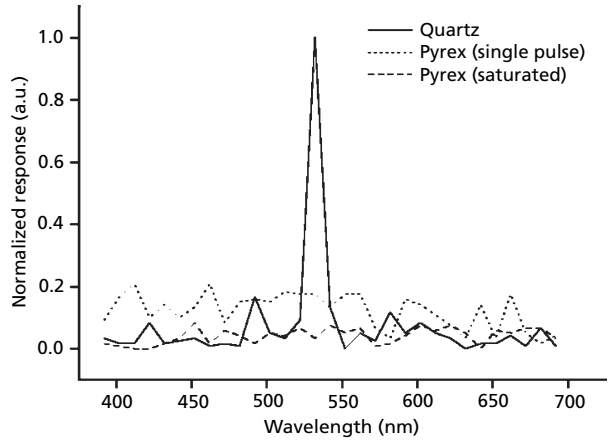

Figure 2 Response spectrum of quartz and Pyrex to a single laser pulse and after 10 s of laser irradiation. Each measurement was the average of ten scans and particle size was 125–180 μm. The data were all normalized to the peak SHG intensity.

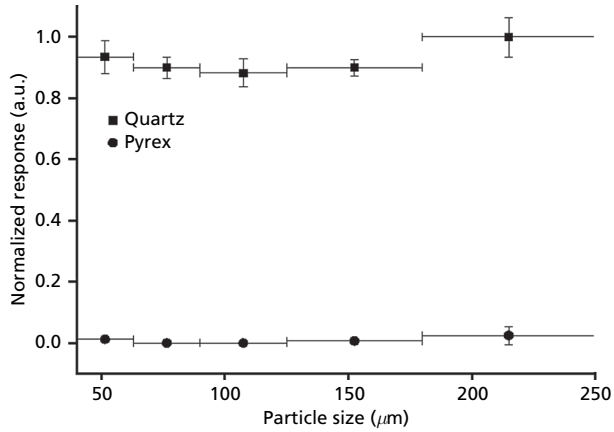

Figure 3 Second harmonic response of different particle size ranges of quartz and Pyrex (mean ± s.d. (y-axis), n = 3). x-axis error bars represent particle size ranges.

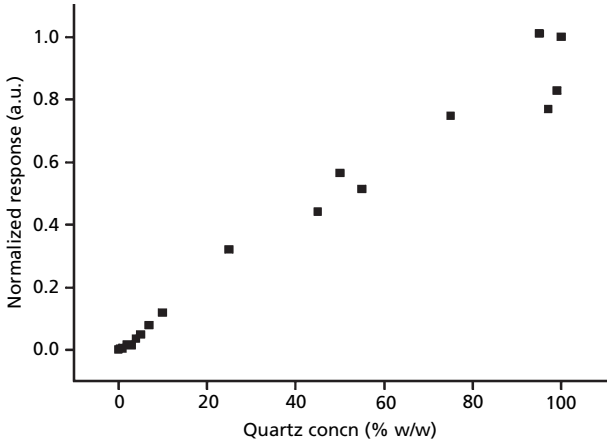

Figure 4 Second harmonic response of binary mixtures of quartz and Pyrex as a function of increasing quartz concentration. Particle size was 90–125 μm and samples were irradiated for 30 s before measurement.

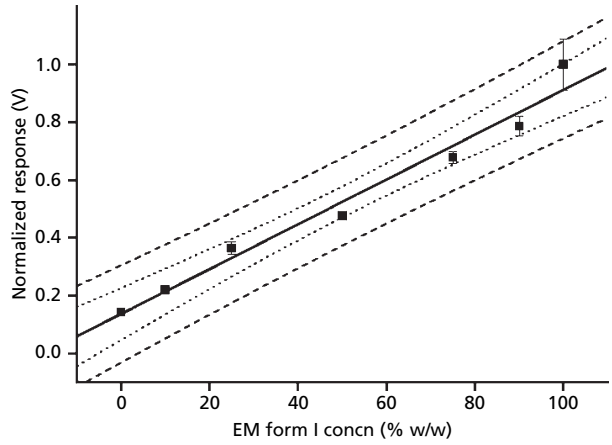

Figure 5 Second harmonic generation from binary mixtures of enalapril maleate (EM) forms I and II with 95% confidence bands (dots) and prediction bands (dashes) (mean ± s.d., n = 3). The particle size range was < 63 μm.

Pyrex exhibited a minimal response over the entire size range as expected (Strachan 2005).

The SHG response to mixtures of quartz and Pyrex is shown in Figure 4. The intensity of scattered SHG light was expected to depend linearly on quartz concentration. This appeared to be true at low quartz concentrations. However, for samples with quartz concentrations above 50% the standard deviation of the response increased. Recent work has shown that the high standard deviation obtained at high percentages of the more active compound was due to the particular experimental geometry employed in these experiments (Rawle et al 2006). The results shown in Figure 4 indicated that the second harmonic intensity depended on the number density of quartz alone. Glass is amorphous, thus to first order, does not have a second-order nonlinearity and emits no radiation at the second harmonic wavelength. Thus the amount of SHG radiation measured depends only on the number of quartz particles contained within the area of the laser beam.

Pharmaceutical materials

To demonstrate the utility of the technique in pharmaceutically interesting examples the response, size dependence and concentration dependence of enalapril maleate (EM) forms I and II and povidone (polyvinylpyrrolidone) are described. Mixtures of lactose polymorphs were also investigated. Experimental details of these applications are presented in Strachan et al (2004b, c).

Quantification of binary polymorphic mixtures The intensity of SHG light from binary mixtures of enalapril maleate forms I and II should depend linearly on the concentration of form I with an intercept that depends on the response of pure enalapril maleate form II. Regression analysis of the data shown in Figure 5 showed a significant relationship between form I concentration and measured SHG intensity ($P < 0.0001$). The non-zero intercept ($P = 0.012$) was expected from the response obtained in Figure 5. As with the quartz Pyrex measurements, at low concentrations of the more active component (form I) the standard deviations of the responses were small; however as the proportion of form I increased, the standard deviation of measurements increased.

Calculation of the limit of detection (LOD) based on the standard deviation of the slope derived from a linear fit (response = 0.0078(% form 1) + 0.14, $r^2 = 0.974$) resulted in an LOD of 23.5%. However, if the LOD was calculated based on the standard deviation of the three 0% form I values, the LOD became 5.1%. This decrease in LOD was probably due to the large standard deviations of the responses at high form I concentrations. At present the LOD values are unacceptably high for practical use, however, with experimental improvement the technique may provide acceptable LOD values for in-line process control.

At present the measurements are limited by the signal-to-noise ratio of the apparatus, rather than any fundamental limitation. The amount of signal can be improved by collecting a larger fraction of light emitted by the sample (see Rawle et al 2006). More signal over a wider range of wavelengths can be generated by using a more appropriate laser source with a shorter pulse duration and correspondingly higher intensity; these lasers have been employed in many surface SHG spectroscopic studies and such experiments have demonstrated sensitivity to extremely low concentrations of the chemical under study (Marrucci et al 2002).

Quantification of crystalline/amorphous mixtures Enalapril maleate form II and povidone mixtures are an example of mixtures of materials that are crystalline and amorphous. Although these are chemically dissimilar and therefore easy to distinguish, this technique can be more generally applied since amorphous materials cannot emit SHG radiation. This example provides an excellent proof of principle of the main strength of SHG measurements—to determine accurately and quickly the contamination by crystalline material of an otherwise amorphous substance. From Figure 6, it can be seen that the second harmonic response increased with increasing enalapril maleate form I concentration ($P < 0.001$), although the fit indicated a non-zero intercept, that was likely to be due to noise ($P = 0.534$).

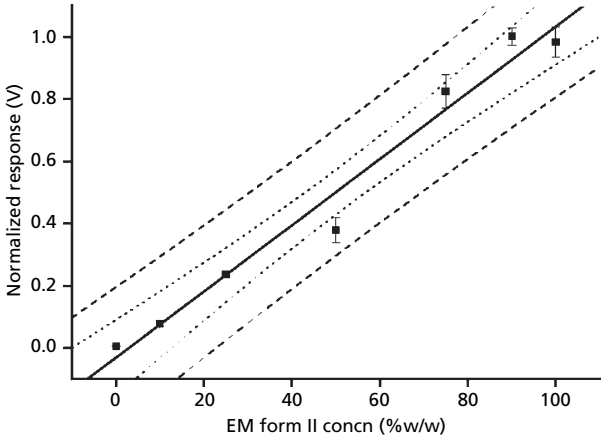

Figure 6 Second harmonic generation from binary mixtures of enalapril maleate (EM) form II and PVP with 95% confidence bands (dots) and prediction bands (dashes). The data points and error bars were the mean and standard deviation from three measurements. The particle size range was 0–63 μm.

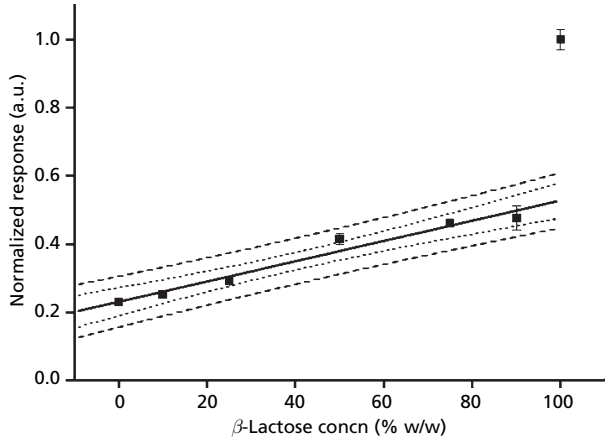

Figure 7 Second harmonic generation from binary mixtures of β-lactose in α-lactose monohydrate with 95% confidence bands (dots) and prediction bands (dashes). The data points and error bars were the mean and standard deviation from three measurements. Particle size range was 63–125 μm. The linear fit was calculated using the second harmonic response from 0 to 90% β-lactose.

The LOD values were 23.0% and 0.13%, based on the standard deviation of the slope derived from a linear fit (response = 0.01064(% form II) − 0.03165, $r^2 = 0.987$) and three 0% form II values, respectively. The very great discrepancy between the two values suggested that use of SHG was an excellent technique to detect small amounts of crystalline enalapril maleate form II in an otherwise amorphous povidone medium. However, at higher levels of crystallinity the technique requires an improved experimental geometry.

The LOD of 0.13% is substantially lower than levels obtained using most other techniques, such as near-infrared spectroscopy and X-ray powder diffraction (Tanninen & Yliruusi 1992; Giron et al 1999; Patel et al 2000, 2001; Dong et al 2002). Although further investigations are required, including those on a crystalline and amorphous form of the same pharmaceutical substance, the sensitivity to very low levels of crystalline material in an amorphous material and the speed of the technique suggest great potential for quality control of amorphous drug compounds.

Quantification of anhydrate/hydrate mixtures The second harmonic response of binary mixtures of β-lactose and α-lactose monohydrate is shown in Figure 7. There was a linear increase in SHG as the β-lactose concentration increased from 0 to 90%. There was disproportionate increase in SHG at 100% β-lactose which may have been due to β-lactose being a phase-matchable material. If L_c is much larger than r the introduction of the nonphase-matchable α-lactose monohydrate may have disturbed the coherent phase-matched response of β-lactose, leading to a sharp drop in SHG. Up to 90% β-lactose it was likely that no phase-matching occurred. A linear fit in the 0–90% β-lactose concentration range revealed a significant relationship between β-lactose concentration and response ($P < 0.001$). There was a non-zero intercept ($P < 0.001$), which confirmed that pure α-lactose monohydrate produced a significant second harmonic response (Strachan et al 2004b; Strachan 2005). Quantitative analysis of the data yielded LOD values of 24.9% and 12.7% based on the standard deviation of the slope (0 to 90% β-lactose) and 0% β-lactose sample measurements, respectively.

Influence of particle size on SHG Figure 8 shows the particle size dependence of the nonlinear response of enalapril maleate forms I and II and povidone. As expected, povidone did not exhibit a significant response at any size range. Enalapril maleate form I exhibited the most intense overall response and was dependent on particle size ($P = 0.002$, where P is the chance of the result occurring randomly) with the peak response occurring in the 90–125 μm size range. Enalapril maleate form II also showed a significant nonlinear response although it was less intense than that of form I. The SHG response of enalapril maleate form II was also dependent on particle size ($P = 0.040$) with the peak response occurring

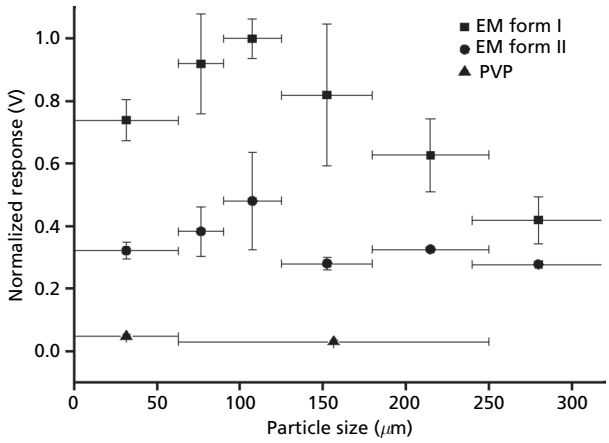

Figure 8 Second harmonic response of different particles size ranges of enalapril maleate (EM) forms I and II and povidone. Data points and y-axis error bars were the mean and standard deviation of three measurements. Error bars on x-axis represent particle size ranges.

in the 90–125 μm size range. The statistical analysis of the particle size dependence was by using a one-way analysis of variance combined with the Tukey method (95% confidence level) of mean comparisons (Strachan 2005).

The size dependence of the SHG emitted from a particular material depends on the polymorph of the material and its optical properties. Essentially, this comprises a measurement of the polarization dependence of the material's refractive index at both the fundamental and the second harmonic wavelengths. In general, and as shown in Figure 1, once the particle size is over a particular threshold value, no size dependence will be observed (e.g. in quartz as shown above). However, below this threshold value size dependence will be observed. The size dependence also changes with the phase matching behaviour of the material, as shown in Figure 1.

Angular dependence of SHG Recently, measurements of the bulk SHG response as a function of both angle of incidence and angle of measurement have been performed (see Figure 9) (Rawle et al 2006). These measurements, along with control over the amount of sample illuminated, have provided lower values for the LOD and LOQ for crystalline–crystalline mixtures, while also having the potential to provide simultaneous particle size information, thus eliminating any potential problem with particle size dependence on the measurements.

The laser illuminates a circle of radius 1.5 mm, which is much larger than the particle size. Thus, it is expected that the optical nonlinear response will be a smooth function of the angle as shown in Figure 10. Note that the shape of the intensity vs angle plot was independent of particle size, while the absolute magnitude of the response was strongly dependent

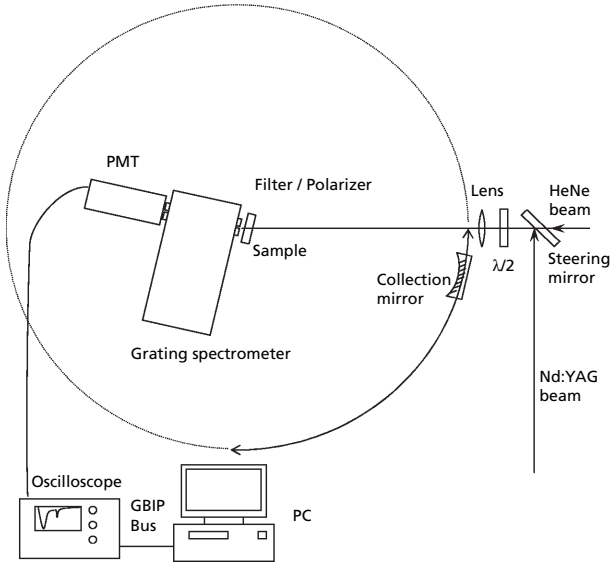

Figure 9 Apparatus for detecting optical scattering as a function of angle of incidence and angle of measurements. The geometry of the apparatus is such that as the collection mirror rotates about the sample it is always directing light into the entrance slit of the spectrometer at the correct angle of incidence. The laser beam is maintained at a fixed angle of incidence to the sample though out the measurement.

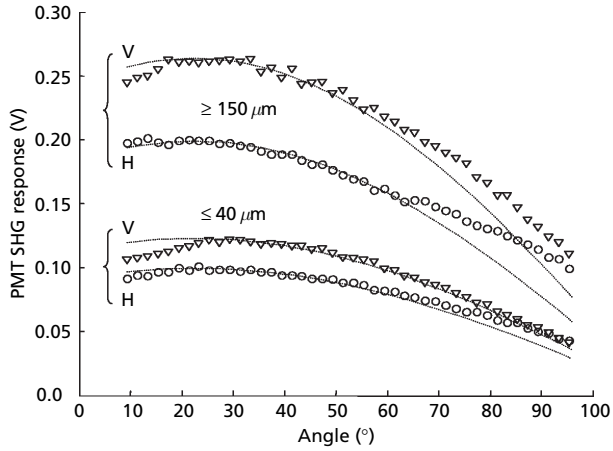

Figure 10 Particle size and polarization dependence of second harmonic generation (SHG) from lactose. The fitted curves were the expected angular dependence from purely geometric optics considerations.

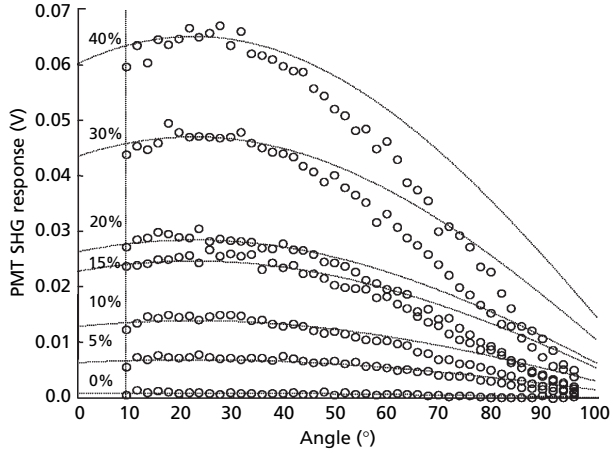

Figure 11 Scattering intensity for varying percentages of enalapril maleate form II. The fitted curves were the expected angular dependence from purely geometric optics considerations.

on particle size. However, upon analysing the polarization dependence of the scattered light it was found that the angle of peak response was weakly dependent on particle size, which was unexpected and requires further investigation.

Measurements on enalapril maleate form II/povidone mixtures similar to those presented in Figure 6 have been performed using variable angle measurements as described (Figure 11) (Rawle et al 2006). The LOD (already excellent) was not improved by this method, however the accuracy of quantification was improved at higher percentages.

Comparison with other spectroscopic methods

The use of second-order nonlinear optical properties as a method for characterizing bulk materials has been of little interest until recently. However, such experiments have now proved to be a fruitful vein of research, particularly as a method for aiding the characterization of bulk and often

turbid media, and more often surfaces and interfaces. SHG in bulk materials is complementary to existing spectroscopic methods such as infrared (IR) and near-infrared, and Raman spectroscopy. The technique is in its infancy, and thus it is difficult to definitively state its advantages and disadvantages compared with other spectroscopic methods. However, some conclusions can be drawn, both from theory and practice. In contrast to IR, near-IR and Raman spectroscopy the technique is insensitive to all liquids and gases (either polar or nonpolar), and hence atmospheric components such as water and carbon dioxide do not interfere with measurements. In contrast to IR spectroscopy, the method requires no sample preparation. It has been shown that SHG can be used to detect very low levels of polymorphism or crystallinity, probably lower than the levels which can be detected by other rapid spectroscopic methods.

Like other spectroscopic methods, SHG is sensitive to phase transitions and provides quantitative information on those phase transitions. By utilizing a tuneable laser source, potentially complex mixtures with more than two phases could be investigated, however, some *a priori* knowledge of the system would be necessary to interpret the information received. Finally, the processing speed of SHG experiments is very fast, potentially ms or less, limited only by the pulse repetition rate of the laser. Thus bulk SHG measurement techniques have many of the qualities desirable for industrial monitoring of pharmaceutical processing. Practical considerations such as issues with interfacing the system with a process have not been thoroughly investigated. However, similar issues to those for other spectroscopic methods such as near-IR and Raman spectroscopy would be expected.

Conclusion

A variety of spectroscopic and other techniques are used to characterize bulk materials and systems, including those in the pharmaceutical sciences. Nevertheless, many complex organic systems remain difficult to investigate and monitor, due to a lack of appropriate analytical techniques. Therefore, there is continued interest in improving existing spectroscopic methods and using novel spectroscopic approaches to characterize biological and pharmaceutical systems.

Second-order nonlinear optical processes, including SHG, depend on the spatial arrangement of molecules as well as the chemical structure of the molecules themselves. It has been shown to be useful in investigating and quantifying bulk properties including phase changes and mixture ratios. The physical response is very fast (instantaneous), thus measurement speed is limited only by the apparatus used to make the measurements. There is ample scope for improving existing apparatus which makes this technique an attractive option for in-line quantitative control in industrial processes.

Recent research has suggested that nonlinear optical response may be a viable tool for obtaining physicochemical information about systems and monitoring such systems during industrial processes. The development of methods to probe second-order optical nonlinear processes for such purposes will be watched with interest.

References

Aaltonen, J., Rantanen, J., Siiria, S., Karjalainen, M., Jorgensen, A., Laitinen, N., Savolainen, M., Seitavuopio, P., Louhi-Kultanen, M., Yliruusi, J. (2003) Polymorph screening using near-infrared spectroscopy. *Anal. Chem.* **75**: 5267–5273

Akagawa, K., Wada, S., Tashiro, H. (1997) High-speed optical parametric oscillator pumped with an electronically tuned Ti:sapphire laser. *Appl. Phys. Lett.* **70**: 1213–1215

Amidon, G. L., Lennernäs, H., Shah, V. P., Crison, J. R. (1995) A theoretical basis for a biopharmaceutic drug classification: The correlation of in vitro drug product dissolution and in vivo bioavailability. *Pharm. Res.* **12**: 413–420

Baxter, G. W., He, Y., Orr, B. J. (1998) A pulsed optical parametric oscillator, based on periodically poled lithium niobate (PPLN), for high-resolution spectroscopy. *Appl. Phys. B* **67**: 753–756

Bernstein, J. (2002) Polymorphism in molecular crystals. *International Union of Crystallography, Monographs on Crystallography*. Oxford University Press, Oxford

Blanco, M., Coello, J., Iturriaga, H., Maspoch, S., De La Pezuela, C. (1998) Near-infrared spectroscopy in the pharmaceutical industry. *Analyst* **123**: 135R–150R

Boyd, R. W. (1992) *Nonlinear optics*. 1st edn, Academic Press, San Diego

Brittain, H. G. (1995) (ed.) *Physical characterization of pharmaceutical solids*. Marcel Dekker, Inc., New York

Brittain, H. G. (1999a) *Polymorphism in pharmaceutical solids*. Marcel Dekker Inc., New York

Brittain, H. G. (1999b) *Polymorphism in pharmaceutical solids*. Marcel Dekker Inc., New York, pp 281–282

Brittain, H. G. (1999c) *Polymorphism in pharmaceutical solids*. Marcel Dekker Inc., New York, pp 355–356

Carstensen, J. T. (1977) *Pharmaceutics of solids and solid dosage forms*. John Wiley and Sons, New York

Center for Drug Evaluation and Research (CDER) (2000) *Guidance of industry; waiver of in vivo bioavailability and bioequivalence studies for immediate-release solid oral dosage forms based on a Biopharmaceutics Classification System*. US Department of Health and Human Services, pp 2–4

Colthup, N., Daly, L., Wiberley, S. (1990) *Introduction to infrared and Raman spectroscopy*. Academic Press, Inc., San Diego

Dong, Z. D., Munson, E. J., Schroeder, S. A., Prakash, I., Grant, D. J. W. (2002) Neotame anhydrate polymorphs II: quantitation and relative physical stability. *Pharm. Res.* **19**: 1259–1264

Fokin, Y. G., Krupenin, S. V., Murzina, T. V., Aktispetrov, O. A., Soria, S., Marowsky, G. (2004) Ferroelectric switching and phase transitions in thin cells of chiral smectic liquid crystals. *Surf. Sci.* **566–568**: 783–788

Giron, D., Piechon, P., Goldbronn, S., Pfeffer, S. (1999) Thermal analysis, microcalorimetry and combined techniques for the study of the polymorphic behaviour of a purine derivative. *J. Therm. Anal. Cal.* **57**: 61–73

Haleblian, J. K. (1975) Characterization of habits and crystalline modification of solids and their pharmaceutical applications. *J. Pharm. Sci.* **64**: 1269–1288

Haleblian, J. K., McCrone, W. (1969) Pharmaceutical applications of polymorphism. *J. Pharm. Sci.* **58**: 911–929

Hancock, B. C., Zografi, G. (1997) Characteristics and significance of the amorphous state in pharmaceutical systems. *J. Pharm. Sci.* **86**: 1–12

Henson, B. F., Asay, B. W., Sander, R. K., Son, S. F., Robinson, J. M., Dickson, P. M. (1999) Dynamic measurement of the HMX beta-delta phase transition by second harmonic generation. *Phys. Rev. Lett.* **82**: 1213–1216

Izumi, S., Sato, M., Suzuki, J., Taniuchi, T., Ito, H. (1998) Periodically-poled $LiNbO_3$ optical parametric oscillator with 55% slope efficiency pumped by a *q*-switched Nd:YAG laser. *Jpn. J. Appl. Phys*. **37**: L1383–L1385

Janner, A. M. (1998) *Second-harmonic generation, a selective probe for excitons*. PhD Thesis, University of Groningen, the Netherlands

Kalinkova, G. (1999) Infrared spectroscopy in pharmacy. *Vib. Spec*. **19**: 307–320

Kraus, J. D. (1992) *Electromagnetics*. 4th edn, Mcgraw Hill International Editions, New York

LeCaptain, D. J., Burglund, K. A. (1999) The application of second harmonic generation for in situ measurement of induction time of selected crystallization systems. *J. Crys. Growth* **203**: 564–569

Luner, P. E., Majuru, S., Seyer, J. J., Kemper, M. S. (2000) Quantifying crystalline form composition in binary powder mixtures using near-infrared reflectance spectroscopy. *Pharm. Dev. Tech*. **5**: 231–246

Marrucci, L., Paparo, D., Cerrone, G., De Lisio, C., Santamato, E., Solimeno, S., Ardizzone, S., Quagliotto, P. (2002) Probing interfacial properties by optical second-harmonic generation. *Opt. Las. Eng*. **37**: 601–610

McCeery, R. L. (2000) *Raman spectroscopy for chemical analysis*. John Wiley & Sons, Inc., New York

Miklos, A., Lim, C. H., Hsang, W. W., Liang, G. C., Kung, A. H., Schmohl, A., Hess, P. (2002) Photoacoustic measurement of methane concentrations with a compact pulsed optical parametric oscillator. *Appl. Opt*. **41**: 2985–2993

Patel, A. D., Luner, P. E., Kemper, M. S. (2000) Quantitative analysis of polymorphs in binary and multi-component powder mixtures by near-infrared reflectance spectroscopy. *Intl. J. Pharm*. **206**: 63–74

Patel, A. D., Luner, P. E., Kemper, M. S. (2001) Low-level determination of polymorph composition in physical mixtures by near-infrared reflectance spectroscopy. *J. Pharm. Sci*. **90**: 360–370

Rawle, C. B., Strachan, C. J., Lee, C. J., Manson, P. J., Rades, T. (2006) Towards characterization and identification of solid state pharmaceutical mixtures through second harmonic generation. *J. Pharm. Sci*. **95**: 761–768

Shen, Y. R. (1984) *The Principles of nonlinear optics*. John Wiley and Sons, New York

Son, S. F., Asay, B. W., Henson, B. F., Sander, R. K., Ali, A. N., Zielinski, P. M., Phillips, D. S., Schwartz, R. B., Skidmore, C. B. (1999) Dynamic observation of a thermally activated structure change in 1,3,5-triamino-2,4,6-trinitrobenzene (TATB) by second harmonic generation. *J. Phys. Chem .B* **103**: 5434–5440

Strachan, C. J. (2005) *Spectroscopic investigation and quantitation of polymorphism and crystallinity of pharmaceutical compounds*. PhD Thesis, University of Otago, Dunedin

Strachan, C. J., Pratiwi, D., Gordon, K. C., Rades, T. (2004a) Quantitative analysis of polymorphic mixtures of carbamazepine by Raman spectroscopy and principal components analysis. *J. Raman Spectrosc*. **35**: 347–352

Strachan, C. J., Lee, C. J., Rades, T. (2004b) Partial characterization of different mixtures of solids by measuring the optical nonlinear response. *J. Pharm. Sci*. **93**: 733–742

Strachan, C. J., Rades, T., Lee, C. J. (2004c) Determination of the optical second harmonic response of pharmaceutical solid–solid mixtures. *Opt. Las. Eng*. **43**: 209–220

Sullivan, E. C., Taylor, W. S. (1919) *Glass*. Number 1 304 623. United States Patent Office

Sutherland, R. L. (1996) *Handbook of nonlinear optics*. Marcel Dekker, Inc, New York, pp 207–233

Tang, C. L., Cheng, L. K. (1995) *Fundamentals of optical parametric processes and oscillators*. Volume 20, *Laser science and technology: an international handbook*. Harwood Academic Publishers, Amsterdam

Tanninen, V. P., Yliruusi, J. (1992) X-ray powder diffraction profile fitting in quantitative determination of two polymorphs from their powder mixture. *Int. J. Pharm*. **81**: 169–177

Tishmack, P. A., Bugay, D. E., Byrn, S. R. (2003) Solid-state nuclear magnetic resonance spectroscopy – Pharmaceutical applications. *J. Pharm. Sci*. **92**: 441–474